Determination of Baseline Groundwater Levels for Tree Conservation in Urban Historical Botanical Gardens Using Applied Geophysics

Maria Catarina Paz [1*], Ana Paula Falcão [2], César Augusto Garcia [3], Miguel Esteves [4], Nuno Afonso [1], Maria Paula Mendes [5]

[1] RESILIENCE—Center for Regional Resilience and Sustainability, Escola Superior de Tecnologia do Barreiro, Instituto Politécnico de Setúbal, Rua Américo da Silva Marinho, 2839-001 Barreiro, Portugal
catarina.paz@estbarreiro.ips.pt (MCP)

[2] CERIS, Instituto Superior Técnico, Universidade de Lisboa, Av. Rovisco Pais, 1, 1049-001 Lisboa, Portugal
ana.p.falcao@tecnico.ulisboa.pt (APF);
nunofafonso@tecnico.ulisboa.pt (NA)

[3] Universidade de Lisboa, Museu Nacional de História Natural e da Ciência/ Centre for Ecology, Evolution and Environmental Changes (cE3c). Natural History and Systematics (NHS) Research Group & CHANGE - Global Change and Sustainability Institute, Faculdade de Ciências da Universidade de Lisboa. Rua da Escola Politécnica, 56/58. 1250-102 Lisboa, Portugal
cesargarcia@museus.ulisboa.pt (CAG)

[4] CEG, Instituto de Geografia e Ordenamento do Território, Universidade de Lisboa, Rua Branca Edmée Marques, Edifício IGOT, Cidade Universitária, 1600-276 Lisboa, Portugal
miguele@edu.ulisboa.pt (ME)

[5] CERENA, Instituto Superior Técnico, Universidade de Lisboa, Av. Rovisco Pais, 1, 1049-001 Lisboa, Portugal
mpaulamendes@tecnico.ulisboa.pt (MPM)

[*] Corresponding author

Length of the manuscript: 6551 words (including references and acknowledgements)

Declarations of interest: none.

Funding: This work was supported by the Portuguese Foundation for Science and Technology (FCT) and research units CERIS (UIDB/04625/2020) and CERENA (UIDB/04028/2020); and Instituto Politécnico de Setúbal.

Data availability statement

The data that support the findings of this study are available from the corresponding author upon reasonable request.

Author Contributions

MCP: Formal Analysis, Investigation, Methodology, Resources, Software, Visualization, Writing – original draft, Writing – review & editing;
APF: Methodology, Investigation, Supervision, Writing – review & editing;
CAG: Methodology, Writing – original draft, Writing – review & editing;
ME: Investigation, Resources, Writing – review & editing;
NA: Formal Analysis, Software, Visualization, Writing – original draft;
MPM: Conceptualization, Funding acquisition, Investigation, Supervision, Writing – original draft, Writing – review & editing.

Determination of Baseline Groundwater Levels for Tree Conservation in Urban Historical Botanical Gardens Using Applied Geophysics

Abstract

Historical botanical gardens hold a significant place in cultural heritage. They serve as interpretive repositories of past botanical knowledge and practices, showcase plant collections cultivated over centuries, provide space for the emergence of new ecologies, offer numerous human well-being benefits, and supply vital regulating ecosystem services, which are especially important in urban areas. Nowadays, however, plants within urban historical botanical gardens can be at risk due to urban development. Therefore, it is crucial to achieve a comprehensive understanding of these spaces to help implement protective measures and support proper urban planning of the surrounding areas.

This study investigates the subsurface of the Botanical Garden of Lisbon (JBL), which is subject to nearby construction works that may alter groundwater flow and depth. We employed a methodology designed for minimal on-site disturbance and high adaptability to the spatial constraints typical of these spaces. Two non-invasive applied geophysical techniques were used: electrical resistivity tomography (ERT) and ground-penetrating radar (GPR). Our main objectives were: (1) to assess groundwater levels in the construction area and establish the piezometric surface, and (2) to determine if tree roots reach the saturated zone, establish a groundwater baseline, and suggest protective measures.

The establishment of the piezometric surface and the delimitation of the root zone, extending up to 3.0 m in depth, revealed that tree roots can access groundwater levels. This finding underscores the critical need for vigilant monitoring and management of groundwater levels during excavation activities, as decreased lateral groundwater contributions from the excavation area can adversely affect groundwater levels of trees in the plant beds.

These findings and methodology can be applied to urban botanical gardens worldwide, as many of these gardens face similar challenges due to urbanization and environmental changes.

Keywords:

Historical botanical garden; Groundwater; Roots; Electrical resistivity tomography (ERT); Ground-penetrating radar (GPR); 3D GIS

1 Introduction

Botanical gardens are singular sites of conservation, research, education, and bond with the plant world. They provide numerous human well-being benefits such as aesthetic, artistic, recreational, and spiritual experiences. They also offer vital regulating ecosystem services like carbon storage, heat island mitigation, air pollution removal, and runoff regulation [1–3]. These gardens are connected on a planetary scale through networks where resources, knowledge, and plants are shared, contributing to socio-ecological sustainability and mitigation of biodiversity loss [4].

Many botanical gardens showcase plant collections cultivated over centuries. Notably, they offer a unique opportunity for people to connect with ancient trees, especially as natural landscapes outside cities are progressively replaced by intensive agricultural and forestry operations, energy plants, and new urban, commercial, and industrial zones. Moreover, historical botanical gardens have provided space for the emergence of new ecologies, which interrupt past narratives and open doors to new interpretations of the future of humankind [5].

In contemporary times, the plants in historical botanical gardens are endangered by several factors, such as the climate crisis [1,6–8], military conflicts [9,10], and urban development [11]. Most historical gardens are located within urban landscapes [12], where activities such as excavation work during the building phases of nearby constructions can affect the depth and flow of groundwater [13], soil moisture, tree functions, and the cooling capacity of trees [14–16]. Therefore, careful water management is essential to maintain the physiological processes of plants during the construction phase [1,16].

For this, it is necessary to have a comprehensive understanding of the interactions between tree roots and groundwater through studies that provide detailed information with minimal on-site disturbance. Applied geophysical techniques are particularly appropriate because they are non-invasive, offer high-resolution digital imaging with minimal disruption, and can be selected according to the spatial features of the study areas and the required depth of investigation.

Although interest in the use of digital technologies, such as geographical information systems (GIS) mapping of the ground surface, is gaining momentum in the scope of historical gardens ([14], and references therein), to this day methodologies that include applied geophysical techniques for the characterization of these spaces have not been scientifically reported. In fact, in historical botanical gardens, the spatial layout was planned to provide an immersive didactic experience, with meandering paths of different sizes guiding the public through the plant collection, which makes it difficult to conduct mapping surveys, especially those aimed at investigating and digitally representing the subsurface.

This case study explores the Lisbon Botanical Garden (JBL), a Portuguese historical botanical garden member of Botanic Gardens Conservation International (BGCI) and designated a national monument. JBL faces plans for excavation work related to the construction of a building with cellars in an adjacent area. This construction project has the potential to affect the tree collection, as it may alter groundwater flow and depth. Therefore, it is necessary to gather more knowledge about the root zone to proceed with security. For this, a methodology was applied that considered the spatial layout of the garden features, and the type of soil coverage, which varied from soil in plant beds to pavement coverage on the paths between beds. Two applied geophysical techniques were selected to evaluate tree-root and groundwater depths on different dates, from the beginning of the rainy period to the beginning of the dry period in 2020/21.

Particularly, to assess groundwater levels along the paved paths between plant beds, we used ground-penetrating radar (GPR), which involves transmitting and receiving antennas to record the propagation time of an electromagnetic signal in the subsurface, allowing its visualization. Recent studies have employed GPR to map groundwater table depth along continuous transects. For instance, [17] focused on using GPR to address hydrogeological issues in urban areas, particularly the detrimental effects of rising groundwater levels. [18] reviewed and built a literature database that included cases from all over the world where GPR was employed to assess groundwater levels.

To assess the depth of tree roots in the plant beds, we used electrical resistivity tomography (ERT), which measures the apparent electrical resistivity (Ω m) of the subsurface using electrodes placed at the surface of the ground and then mathematically inverts these values to obtain models of true electrical resistivity to image the subsurface. This technique is suitable for evaluating tree root depth since soil electrical resistivity is sensitive to moisture content, density, lithology, and root presence, and it can be performed with minimal on-site disturbance [19–24]. Electrical resistivity models, or ERT models, can be produced, according to study objectives and available time and budget, in two dimensions (2D) or three dimensions (3D) (e.g., [25]). Their use and layout involve different field setups for data acquisition, which are influenced by study site conditions, such as soil coverage, area, and specific spatial features and constraints, as well as the objectives of the survey. ERT data were acquired in two contiguous plant beds separated by a paved path, producing a 2D ERT model for each plot.

Furthermore, to better understand the root distribution and to present a didactic digital representation of the subsurface, we produced a 3D ERT model in a GIS environment. For this, we used 3D empirical Bayesian kriging (EBK) interpolation [26] instead of the conventional 3D mathematical inversion of ERT data, which demands a specific field setup that was not possible to apply in our study site due to the spatial disposition of the garden. EBK has been considered for several years a robust interpolation methodology that overcomes many of the disadvantages evident in more classic geostatistical models [27]. In addition, EBK has been widely used in several research works, with various themes and different case study applications (such as temperature, soil, rain), as in [28–33]. However, there are no scientific records of the use of EBK for ERT inverted data.

This study provides an appropriate methodology for characterizing historical botanical gardens, facilitating the adoption of protective measures during construction and supporting proper urban planning in surrounding areas.

2. Research aim

In this multidisciplinary study of technological nature, an innovative methodology was developed to investigate the subsurface of historical botanical gardens, tailored to the unique spatial layouts of these spaces

and designed for minimal on-site disturbance. The methodology includes the use of two non-invasive applied geophysical techniques, GPR and ERT, as well as EBK interpolation for the 3D visualization of inverted 2D ERT models. The idea is to acquire relevant knowledge to contribute to the conservation of historical botanical gardens facing excavation works in surrounding areas, aiding in the adoption of protective measures during construction works and in the proper urban planning of the surrounding areas. The main objectives of this work are: (1) to assess groundwater levels within the area of influence of the construction work, aiming to establish the piezometric surface; and (2) to assess whether the roots of trees can reach the saturated zone and determine the groundwater level baseline within the root zone.

3. Materials and methods

3.1 Study site

3.1.1 The garden

JBL, member of the BGSI organization, is located in the heart of Lisbon (Fig. 1), spanning approximately 4 hectares, and was designed in the 19th century to facilitate botanical lessons for the Polytechnic School. Today, the garden is part of the National Natural History and Science Museum – University of Lisbon (MUHNAC/ULisboa) and is designated a national monument.

The garden boasts a vast diversity of species, numbering between 1300 and 1500, from various ecosystems and features a unique microclimate. Meandering paths, streams, waterfalls, and lakes create an immersive experience, transporting visitors to different botanical regions of the world. Among its highlights is a remarkable collection of palm trees, with over 30 distinct species contributing to a tropical ambiance in several sections of the garden. The garden is also home to numerous species of Cycadaceae and Zamiaceae, which are considered living fossils and are crucial for conservation as many are endangered in their natural habitats. Rich in tropical and subtropical species from New Zealand, Australia, China, Japan, Africa, and South America. It also features several internationally recognized and registered large trees, which thrive only in suitable environments,

such as *Ceiba insignis*, *Taxodium mucronatum*, *Sequoia sempervirens* (Fig. 1), *Podocarpus* spp., among others. Since its inception, the garden has engaged in extensive seed and plant exchanges with other institutions, and its first *Index Seminum* was published in 1878. Open to the public since 1878, JBL remains a valuable green space in the heart of Lisbon, continuing its mission of botanical education and conservation [34].

Fig. 1. Location of the study area (a, b, c), meteorological stations (b, c), future excavation area (c), example of tree from the garden collection – *Sequoia sempervirens*, native to the North American west coast (d), view of the contention wall next to the excavation area, with a path coincident with profile GPR1 (e), view of the contention wall with lateral groundwater gallery (f), and detail of the lateral groundwater gallery (d). Aereal images from Google Earth ©.

3.1.2 Climate and geomorphology

According to Köppen classification, Lisbon has a temperate Mediterranean climate, characterized by a dry and hot summer period. Fig. 2 illustrates the precipitation and temperature patterns in Lisbon from 2001 to August 2021 (2001–2020/21), based on data recorded at two meteorological stations operated by the Portuguese Institute for Sea and Atmosphere (IPMA), C1 and C2 (Fig. 1). Notably, precipitation has been increasing in March and decreasing in December, a trend also observed in other regions of Portugal [35]. Additionally, the variability in annual precipitation is growing, fluctuating by more or less than 400 mm per year from the normal. Lastly, the annual maximum temperature is gradually rising.

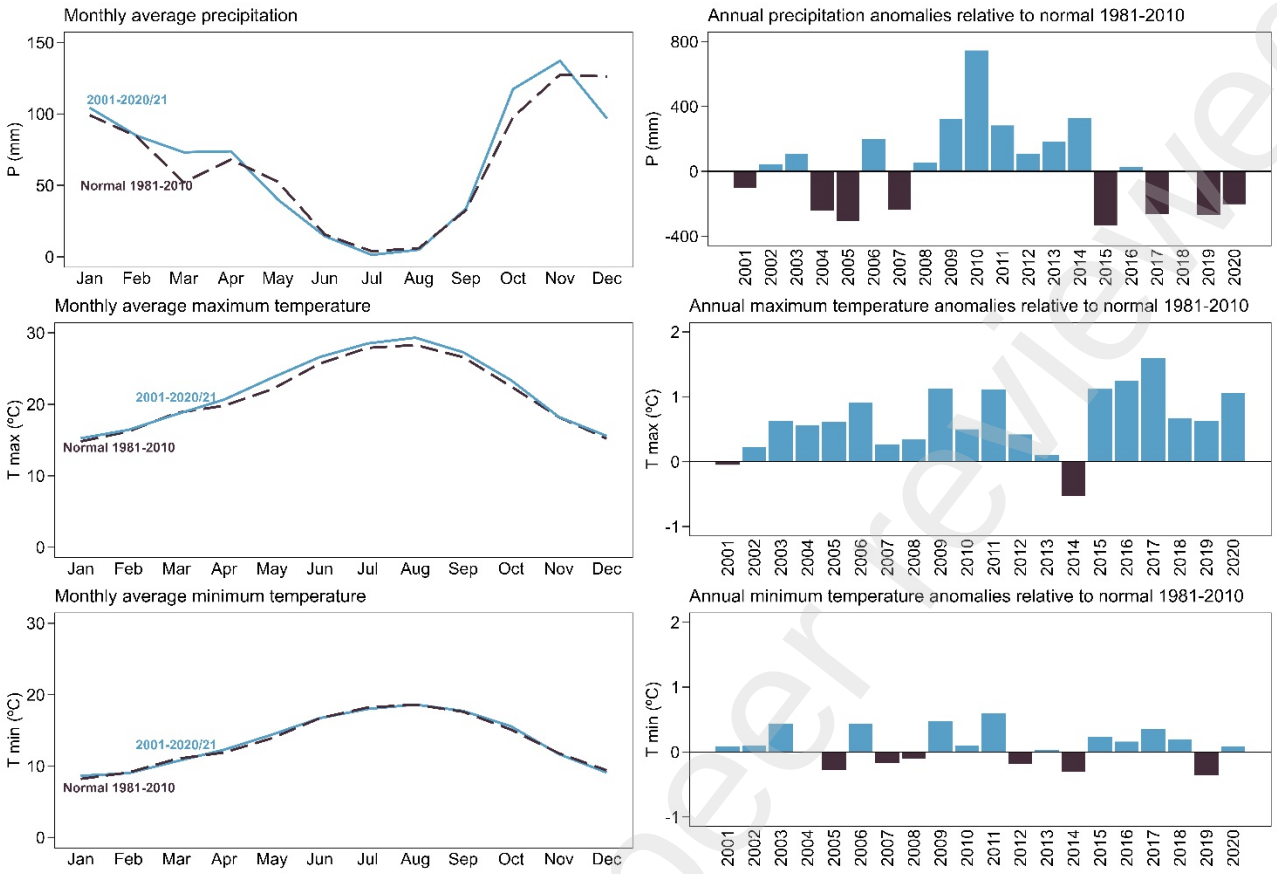

Fig. 2. Characterization of precipitation and temperature in Lisbon for the period from 2001 to August 2021 (2001−2020/21): calculated monthly inter-annual averages and annual anomalies, using data from C1 and C2 meteorological stations operated by the Portuguese Institute for Sea and Atmosphere (IPMA); and 1981−2010 climate normal for C1 (made publicly available by IPMA).

This garden is on a hillslope, with significant changes in elevation, reaching up to 86 m. The highest elevations are observed in the western part of the garden, while the lower elevations are in the northeast, with values around 35 m. A prior geological survey identified an upper substrate made of artificial fill materials that primarily consist of sandy-clayey and clayey materials. Sometimes, they have a higher sand content with fragments or blocks of limestone and basalt, fossil remains, wood, and other artificial elements such as plastic and bricks. This upper substrate has a variable thickness reaching a maximum of 10.0 m to 13.5 m in depth [36]. Beneath the recent deposits lies the Miocene formation of "Argilas dos Prazeres" [37].

The recent upper deposits have interstitial permeability, showing some capacity for water storage, and are recharged by precipitation, by irrigation water via sprinklers, and by seepage from water and sewage distribution network. Our study focuses on this upper layer, which includes the root zone and the phreatic zone. In these artificial deposits, shallow groundwater can circulate according to the topography, generally aligning with the topographical gradient of the garden, flowing from southwest to northeast. However, the heterogeneity of the deposits and the anthropogenically changed urban topography may create localized flow directions different from the general southwest-northeast flow direction. This is the case for the garden zone near the excavation works (Fig. 1), where, following the extreme precipitation event of December 12 and 13, 2022, inputs from south to north were observed, despite the main flow direction generally being southwest to northeast. During this extreme event, precipitation was of 134.6 mm, with 70 mm of this quantity falling in just three hours [38]. Another interesting feature about this zone is the existence of an ancient lateral groundwater gallery that was used in the past, with 2.0 m high and 0.5 m width. This feature is located in the southern extremity of the garden (Fig.1 and Fig. 3), inside a wall that both limits the garden and acts as a contention wall between ground levels.

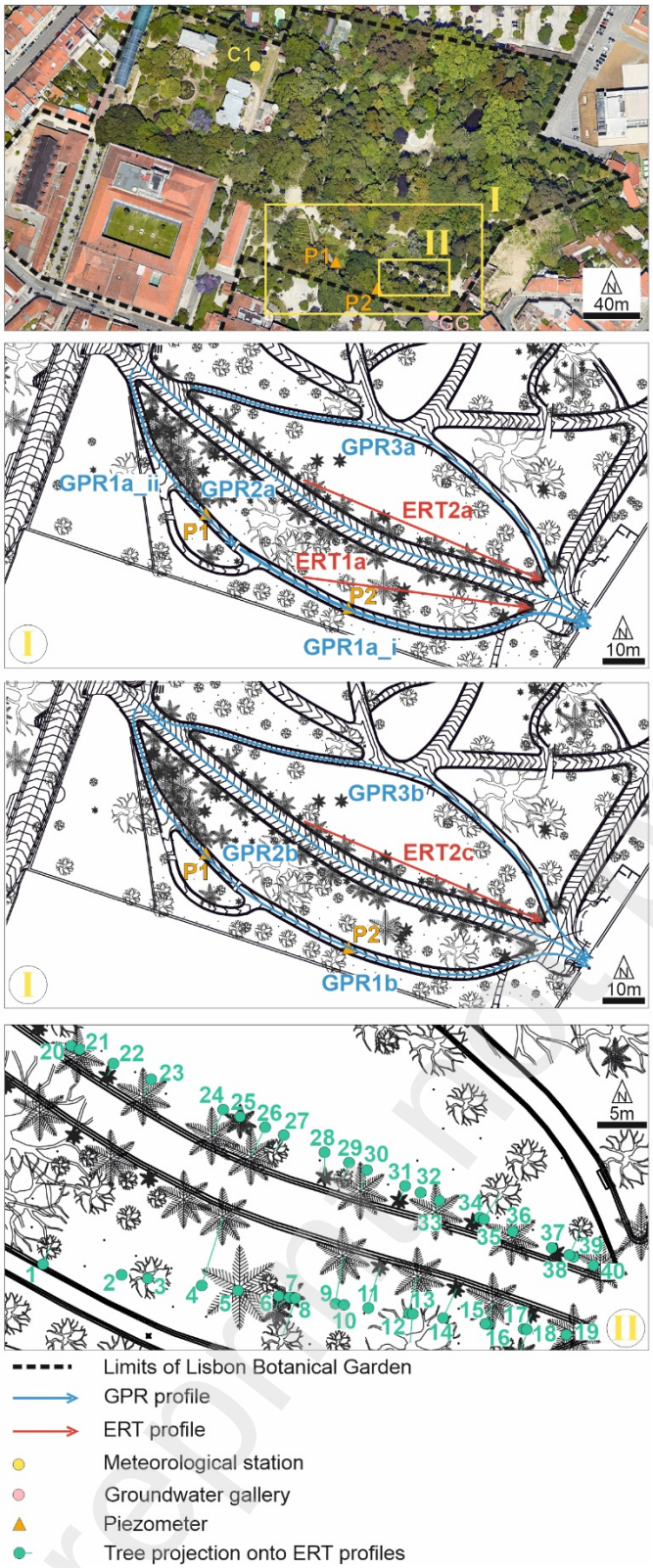

Fig. 3. Location of data acquisition sites and other important features to support interpretation, in Lisbon Botanical Garden. Aereal image from Google Earth ©.

3.2 Methodology

3.2.1 Field data collection

Field surveys were conducted around the two plant beds that potentially can be more affected by the future excavation work, as they are the closest to the construction site (Figs. 1, 3). GPR surveys were conducted in paved paths and ERT surveys in the plant beds (Fig. 3) on the dates specified in Table 1. The study period was comprised in 2020/2021, beginning in October 2020, after a dry period, when groundwater levels are deeper, and ending in June 2021.

Topographic surveys were used to georeference the geophysical data. These were conducted on the profiles where the geophysical data were acquired (Fig. 3), using the marks on the ground where the geophysical equipment was placed, through classic methods (Leica TCR703 Total Station) and global positioning systems (GNSS systems), with a total of 115 points collected. In addition, the elevations of the several points were gathered to generate and enhance the detail of a Digital Elevation Model (DEM) for the entire analyzed area. The final coordinates were presented in the PT-TM06ETRS89 cartographic coordinate system.

Groundwater levels were measured in piezometers P1 and P2 (Fig. 3) using a Seba Hydrometrie level probe, with a precision of 0.005 m, to aid in geophysical and hydrogeological interpretation. P1 has a depth of 12 m and P2 of 13 m.

Table 1- Specifications of geophysical data acquisition. Number suffixes from *1* to *3* refer to spatial location, as in Fig. 3, and letter suffixes from *a* to *c* refer to temporal location of geophysical profiles acquisition, as presented in this table.

ID	Acquisition date	Length (m)	Specifications
GPR1a_i	2020/10/17	86.65	. Equipment: SIR-3000 from GSSI
GPR1a_ii	2020/10/17	49.00	. Antenna: 200 MHz
GPR1b	2021/05/07	138.69	. Antenna setup: common-offset
GPR2a	2020/10/17	122.62	. Mode: time
GPR2b	2021/05/07	122.49	
GPR3a	2020/10/17	114.15	
GPR3b	2021/05/07	127.68	
ERT1a	2020/10/17	54.00	. Equipment: 4point light 10W from LIPPMANN
ERT1c	2021/06/11	54.00	. Array: dipole-dipole
ERT2c	2021/06/11	57.00	. Electrode spacing: 3 m

3.2.2 GPR

GPR is a technique that uses radar pulses, typically in the frequency range of 10 to 1000 MHz, which are transmitted and received by antennas placed on the ground. Different setups of antennas can be used depending on the objective. In this study, we used a common offset setup with a fixed distance between antennas for each profile position. The system measures the time it takes for the radar pulse to travel from emission to reception at each position, creating a radar trace. These traces, when ordered sequentially, form a cross-sectional image of the subsurface known as a radargram. Propagation velocity and amplitude of the electromagnetic signal are controlled by electrical conductivity and dielectric permittivity, which express the response of the materials to electromagnetic fields, and magnetic permeability, which is mostly a function of the presence of ferromagnetic minerals [39]. Penetration depth of the electromagnetic signal decreases with increasing clay content, salinity of the media, and antenna frequency [40–45].

In this study, GPR data were acquired along three profiles (Fig. 3), in two dates −17 October 2020 and 7 May 2021 −using a GSSI SIR-3000 system with a 200 MHz antenna, with specifications as described in Table 1. Data was processed using Reflexw software by Sandmeier. Processing flow consisted essentially of edition of traces, time-zero correction, velocity refinement to 0.15 mm ns^{-1}, background removal, 1D filtering (bandpass butterworth filter maintaining the 70-400 MHz range), and topography introduction.

3.2.3 ERT

ERT is a technique that involves injecting direct current through two electrodes placed on the soil surface, while the voltage between two other electrodes is measured. The disposition of this four-electrode setup changes throughout the profile being investigated, according to the tomographic array chosen, so that a grid of subsoil resistivity values is obtained. These values are then mathematically inverted to obtain models of subsoil electrical resistivity (Ω m) [46], which is the inverse of electrical conductivity. Penetration depth depends on electrical conductivity of subsurface materials, input voltage, and electrodes spacing.

ERT data were acquired along two profiles (Fig. 3), in two dates −17 October 2020 and 11 June 2021 −using a LIPPMANN 4point light 10W system, with the dipole-dipole array [46], which gives good resolution both on vertical and horizontal directions ([47], and references therein), and a 3 m electrode spacing. Specifications are summarized in Table 1.

2D data inversion was carried out with RES2DINV by Geotomo Software, using the robust inversion, with a severe reduction of effects of side blocks in order to minimize their exaggeration due to the robust inversion method [48]. ERT1 data was inverted with electrode spacing reduced to half to minimize the effect of large superficial resistivity variations [48]. Number of iterations of the inversion process was limited to a maximum fixed when the error of each iteration started to tend to a value, so not to create artifacts in the obtained 2D models. Maximum number of iterations was four for ERT1 and ERT2a profiles, and three for ERT2c.

3.2.4 3D EBK interpolation of ERT data

EBK is a robust interpolation methodology which, like other geostatistical models, treats parameters as random variables, reflecting some of their uncertainty, and combines Bayesian theory and kriging interpolation [49]. EBK allows the automation of several procedures to obtain a valid kriging model through a process of dividing the study area into subareas along with multiple simulations, implemented by the iterative estimation of several semi variogram models, which allows to obtain the best possible fit.

For the 3D ERT model construction, ERT1a and ERT2a 2D models, relative to 17 October 2020, were selected. Preliminary processing operations included the manual vectorization of lines for each resistivity class from these models, considering the corresponding depth values. Table data of those lines was processed to assure the proper identification of each class/profile layer, enabling to build a digital surface for each class in both profiles, by using the Triangular Irregular Network interpolation method. As required by the EBK methodology, a grid of orthogonal lines was generated for each profile, with an offset of 5 m, on which the depth for each resistivity class was recorded. For this purpose, a Python script was developed to automate the process of several geoprocessing tools using ModelBuilder in ArcGIS Pro software by ESRI generating 3D grid points. These points

were interpolated using the EBK option of the Geostatistical Analyst toolbox of ArcGIS Pro. The first output is a 3D geostatistical model that calculates and renders itself as a 2D transect at a given elevation. The elevation of the layer was changed using the range slider tool, and the layer updated to show the interpolated predictions for the new elevation. Finally, the EBK model was converted into a voxel (three-dimensional discrete volume unit) layer, resulting on the projected 3D ERT model for 17 October 2020.

4 Results and discussion

4.1 DEM

The DEM shows altitude variations within the area ranging from 55 m to approximately 67 m, with an average altitude of about 59 m. The most prevalent altitude class (37.6%) falls within the range of 54.6 m to 55.6 m, followed by the class spanning 55.6 m to 57.1 m (11.4%). The southernmost plant bed, situated closest to the excavation area (Fig. 1 and Fig. 3), exhibits gentler slopes (3.6−6.6°) compared to the northernmost bed (9.8−13°) (Fig. 3).

4.2 Depth of groundwater level

The piezometric surface was assessed using radargrams obtained from the geophysical campaigns (Fig. 4), and the saturated zone was validated with groundwater level measurements from piezometers P1 and P2 (Fig. 5).

Profiles GPR1a_ii and GPR1a_i, acquired near the contention wall and future excavation area, indicated piezometric levels ranging from 64 to 59 meters at the highest elevations and 59 to 52 meters at the lowest elevations. Profiles GPR2a and GPR3a, situated along the central path and northern path, respectively, showed groundwater levels consistent with those observed in profiles GPR1a_ii and GPR1a_i.

In the second geophysical campaign on 7 May 2021, GPR1b indicated piezometric levels between elevations 62.5 m and 57.5 m, which were 1.5 m lower than those recorded by GPR1a at the higher elevations of the profile. At the lowest elevations of the profile, piezometric levels were either slightly higher or remained the

same. Piezometric levels assessed by GPR2b were approximately 0.5 m higher than those in GPR2a, and piezometric levels assessed by GPR3b were approximately 1 m lower than those in GPR3a.

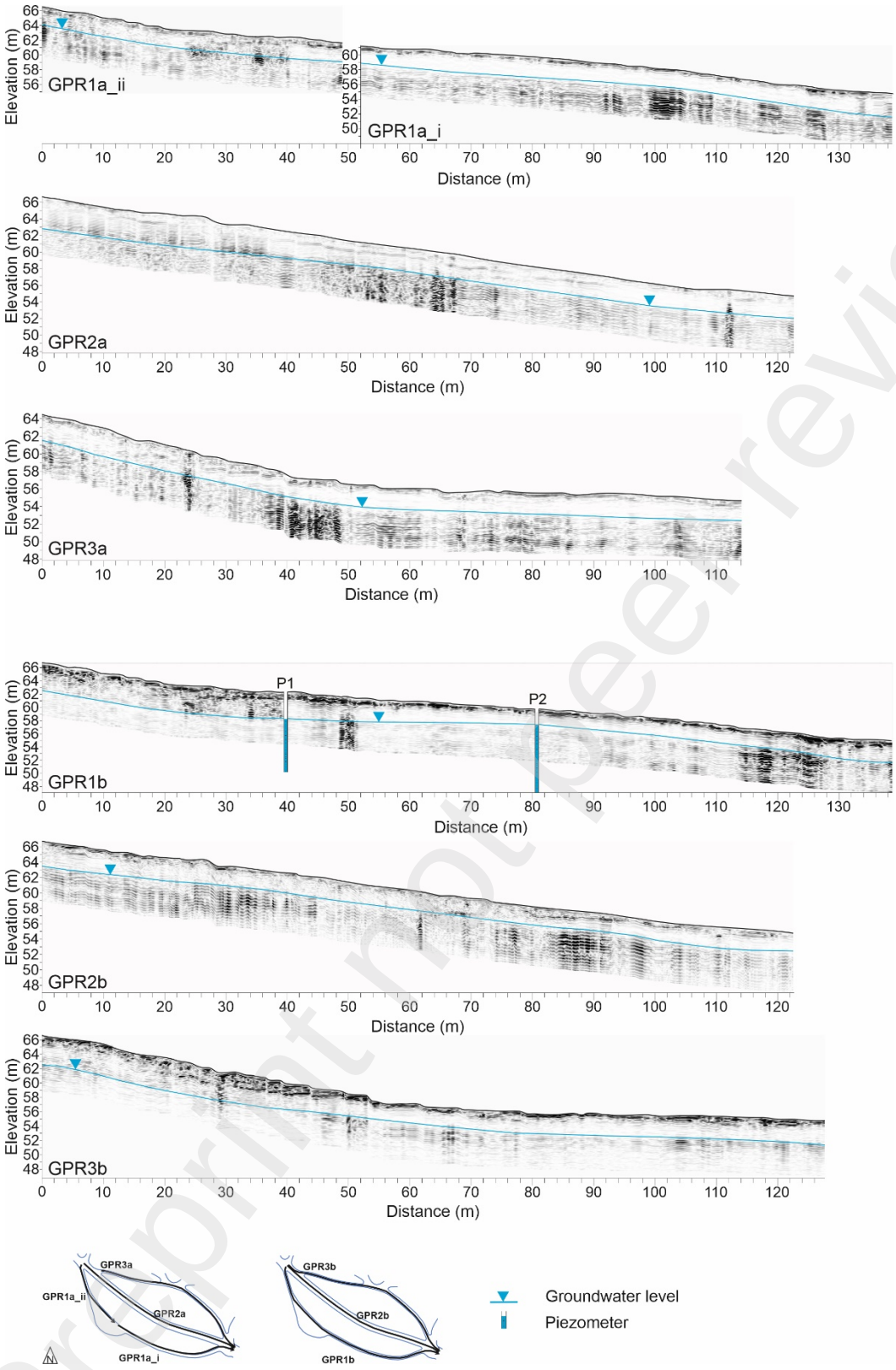

Fig. 4. Ground-penetrating radar (GPR) radargrams with interpreted groundwater level. Groundwater level measured directly with groundwater probe in piezometers P1 and P2.

Fig. 5 shows the monthly temperature and precipitation during the study period, the piezometers used for calibrating the geophysical profiles, and the trends of piezometric levels assessed by GPR in October 2020 and May 2021. The profile located closer to the contention wall (GPR1) exhibited a negative trend in piezometric levels in the upper zone and a positive trend in the lower zone (Fig. 5c). GPR2, situated between the two studied plant beds, showed a positive trend, while GPR3 displayed a negative trend in piezometric levels on both dates.

GPR1 is located in an area with the highest density of irrigation sprinklers (Fig. 5c), which are more concentrated at lower elevations and near the groundwater gallery (Fig. 3). This appears to influence groundwater levels in this area, suggesting that irrigation contributes to localized recharge while also hinting at a south-north flow contribution from the future excavation area. Additionally, piezometric levels measured at piezometers P1 and P2 dropped from May to June 2021 (Fig. 5b), indicating that precipitation is the main contributor to recharge, as the ongoing irrigation was insufficient to prevent the decrease in piezometric levels. In the case of GPR2, it consistently showed a rise, as the plant beds drained towards it. GPR3 is the least influenced by irrigation because of the sprinkler's location, and, therefore, was more dependent on recharge from precipitation.

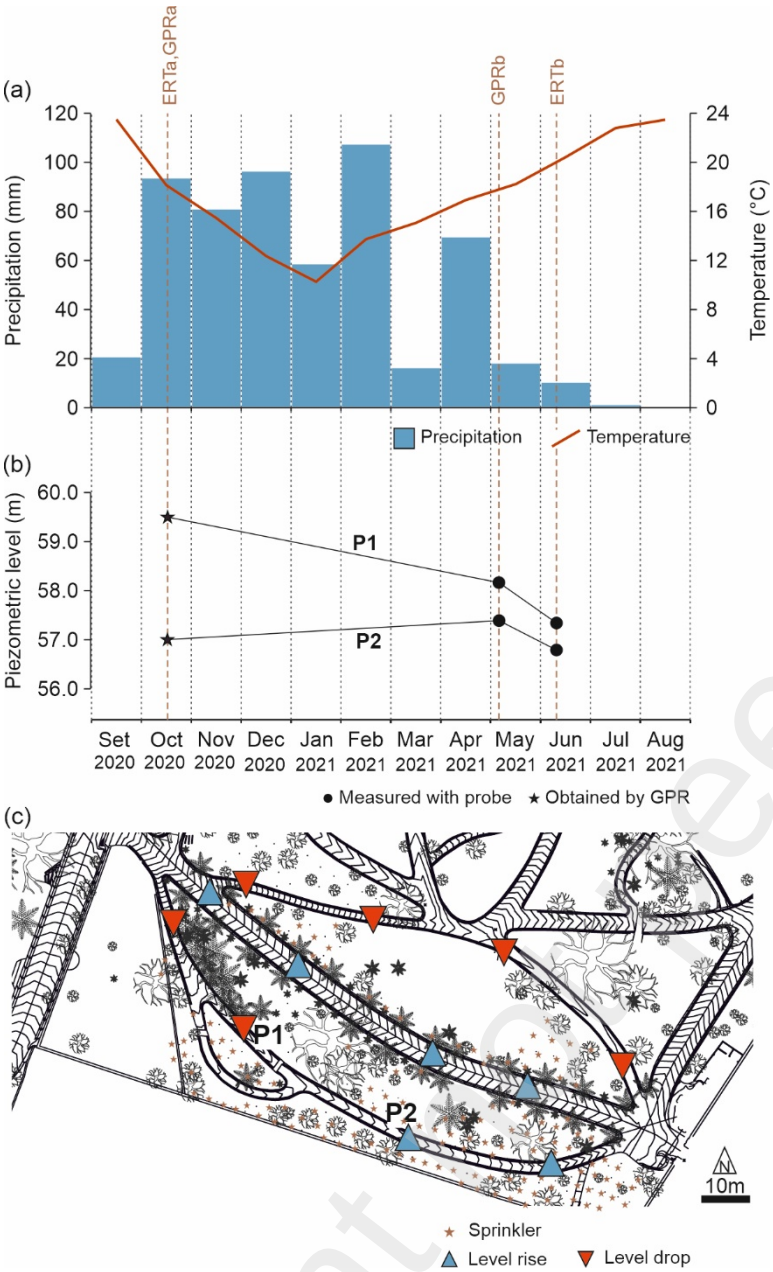

Fig. 5. For the study period September 2020 to August 2021: a) monthly precipitation and monthly mean temperature recorded at C1 meteorological station operated by the Portuguese Institute for Sea and Atmosphere (IPMA); b) piezometric levels assessed at piezometers P1 and P2; and c) trend of piezometric levels from 17 October 2020 to 07 May 2021.

4.3 Depth of tree roots

Fig. 6a presents the obtained 2D ERT models relative to 17 October 2020 (ERT1a and ERT2a) and to 11 June 2021 (ERT2c). Both ERT1 and ERT2 reached a depth of approximately 8 m, which places them within the upper substrate

composed of artificial fill materials (Section 2.3). In general, the electrical resistivity values are below 140 Ω m, which is consistent with the presence of sandy-clayey and clayey materials, as reported by [36] for the area.

Closer to the soil surface, the ERT2a and ERT2c profiles revealed a spatial pattern of electrical resistivities ranging from 40 Ω m to 140 Ω m, reaching a maximum depth of approximately 4 m with little variation over time. The spatial distribution of this pattern aligns with similar studies that used ERT to identify the root zone [20–23,50], suggesting that this zone corresponds to the root zone of the trees in the northernmost plant bed. A similar resistivity pattern was observed in ERT1a, at the southernmost bed, indicating that the root zone there extends to depths of 2.5 to 3.0 m. This suggests that tree roots in the northernmost bed go deeper. The shapes identified within the root zone in each profile may reflect the different tree species, as each has its own characteristic spatial distribution. For example, the high-resistivity zone in the upper part of ERT2 appears to be associated with tree 23, visible in both periods (ERT2a and ERT2c).

In terms of the contrast between the electrical resistivity of the substrate and the root zone, similar patterns have been observed in previous studies [22] and [23], where a lower resistivity layer contrasts with a higher resistivity top layer corresponding to the root zone.

Groundwater levels identified with GPR on the same date were incorporated into the ERT1a and ERT2a profiles, confirming that, at that time, the groundwater levels reached the zone identified as the root zone. In ERT2c, we can analyse the temporal alteration of spatial patterns of electrical resistivity and verify that in the area identified as the root zone, there is some variation in resistivity values. This variation is due to changes in soil moisture related to weather season. From October 2020 to June 2021, a decrease in resistivity values was noticed in the lower zone of the ERT2 profile, passing from classes 20–40 Ω m and 40–60 Ω m to the class 0–20 Ω m. This decrease might be related to the increase in soil water content, at the end of the rainy period (Fig. 5).

Fig. 6b shows the 3D ERT model, obtained by EBK interpolation based on the 2D ERT models, relative to 17 October 2020. In this 3D GIS representation, the interpretation of the tree root zone from the 2D ERT models has been incorporated, providing a clearer visualization of the subsurface beneath and between the two profiles,

and, by extension, the two garden beds analyzed. The tree root zone is visible near the soil surface, and the spatial arrangement of the higher resistivity zone in the upper region, particularly near the northernmost bed, which was already identified in the 2D ERT profiles, is clearly seen. When comparing this representation with the tree layout shown in Fig. 3, it becomes evident that this subsurface zone is associated with the higher concentration of plants.

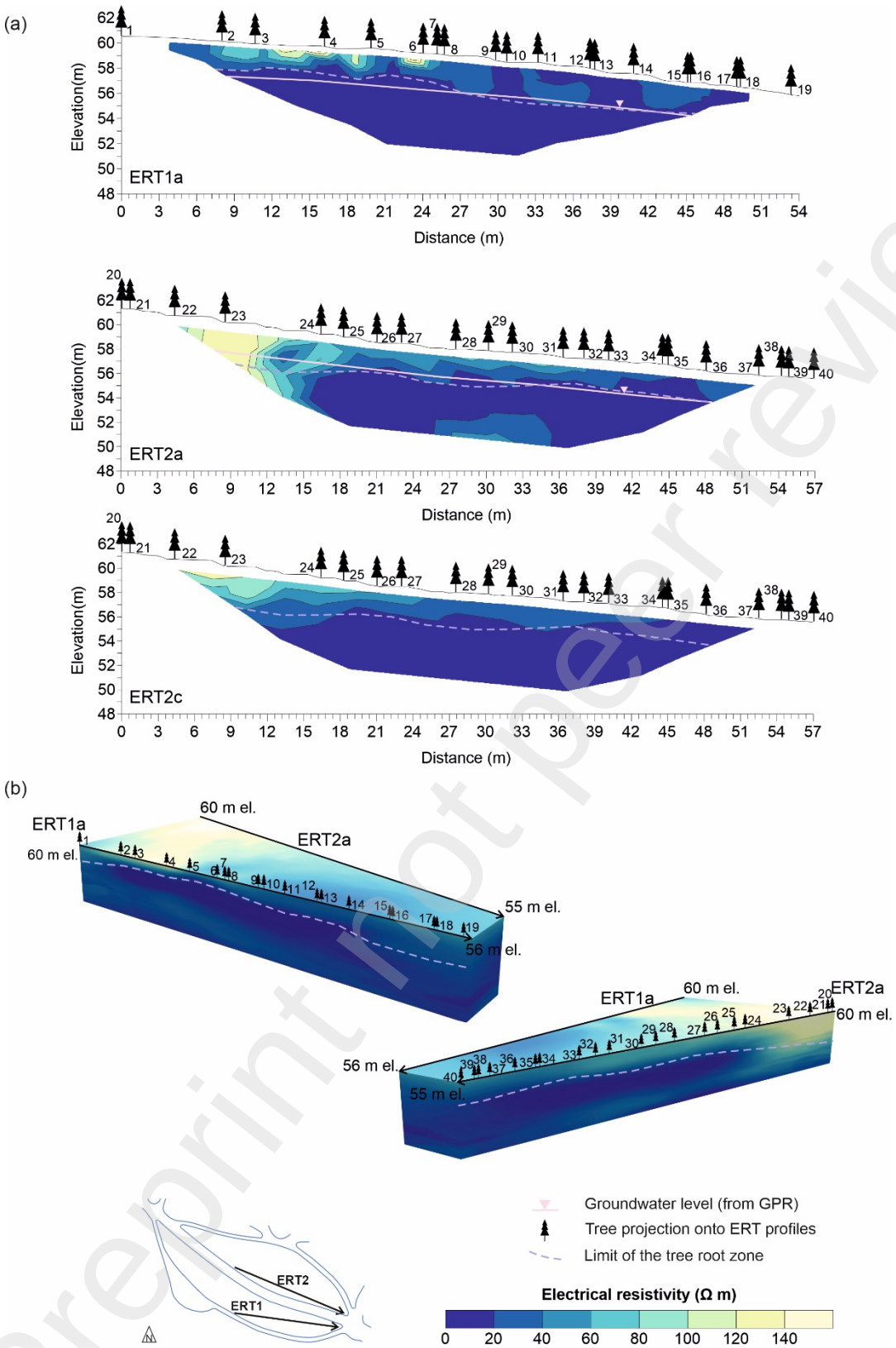

Fig. 6. Electrical resistivity tomography (ERT) models with tree root zone interpretation: a) 2D ERT models; and b) two side views of the 3D ERT model, obtained by EBK interpolation based on the 2D ERT models, for the first date of ERT data acquisition, 17 October 2020. 'el.' stands for elevation.

5 Conclusions

In this study, a methodology based on the use of two non-invasive geophysical techniques, ERT and GPR, was employed to map tree root systems and groundwater levels in a historical botanical garden with spatial constraints located in an urban landscape environment. Based on the comprehensive analysis of the obtained ERT models and GPR radargrams, along with piezometric, meteorological, and spatial feature information, the following main conclusions can be drawn.

The establishment of the piezometric surface and the delimitation of the root zone (up to 3.0 m depth) for the two geophysical acquisition dates, corresponding to rainy and dry periods, revealed that tree roots indeed reach groundwater levels. This indicates that the baseline groundwater levels within this area are close to the surface, even during the study period, which was classified as dry and warm. Although localized recharge from irrigation occurs, precipitation remains the primary source of groundwater recharge. This underscores the critical need for vigilant monitoring and management of groundwater levels during excavation work, as decreasing lateral groundwater contributions from the future construction area may adversely impact groundwater levels within the two study plant beds.

To maintain baseline conditions, with groundwater levels around 3 m, it is recommended to monitor and study groundwater levels closely during construction. Installing wireless dataloggers at piezometers P1 and P2 will enable continuous recording and remote data communication of groundwater levels and temperature, ensuring effective management of groundwater conditions during the construction works.

These results show the effectiveness of combining non-invasive geophysical techniques, specifically ERT and GPR, to map tree root systems and groundwater levels in historical botanical gardens, providing detailed information with minimal on-site disturbance and high adaptability to the spatial constraints. Moreover, incorporating 2D ERT data into a 3D GIS environment not only aided visualization but also made it easier for non-

experts to grasp the subsurface conditions. Additionally, the EBK geostatistical interpolation method offered an effective alternative for visualizing inverted 2D ERT data in a 3D mode. Thus, the methodology developed in this study can be replicated in spaces with similar constraints. Furthermore, the results obtained are relevant to urban botanical gardens globally, given that many of these gardens encounter comparable challenges from urban development and environmental shifts.

Acknowledgements

The authors are grateful to Instituto Dom Luiz, University of Lisbon, Portugal, for providing the geophysical equipment, and to Dr. Marta Lourenço, director of the National Museum of Natural History and Science of the University of Lisbon (MUHNAC).

References

[1] E. Carrari, C. Aglietti, A. Bellandi, C. Dibari, F. Ferrini, S. Fineschi, P. Galeotti, A. Giuntoli, R. Manganelli Del Fa, M. Moriondo, M. Mozzo, G. Padovan, C. Riminesi, F. Selvi, M. Bindi, The management of plants and their impact on monuments in historic gardens: Current threats and solutions, Urban For. Urban Green. 76 (2022) 127727. https://doi.org/10.1016/j.ufug.2022.127727.

[2] N. Othman, N. Mohamed, M.H. Ariffin, Landscape Aesthetic Values and Visiting Performance in Natural Outdoor Environment, Procedia - Soc. Behav. Sci. 202 (2015) 330–339. https://doi.org/https://doi.org/10.1016/j.sbspro.2015.08.237.

[3] R. Rostami, H. Lamit, S.M. Khoshnava, R. Rostami, M.S.F. Rosley, Sustainable Cities and the Contribution of Historical Urban Green Spaces: A Case Study of Historical Persian Gardens, Sustainability 7 (2015) 13290–13316. https://doi.org/10.3390/su71013290.

[4] K.G. Neves, Botanic Gardens in Biodiversity Conservation and Sustainability: History, Contemporary Engagements, Decolonization Challenges, and Renewed Potential, J. Zool. Bot. Gard. 5 (2024) 260–275. https://doi.org/10.3390/jzbg5020018.

[5] M. Boehi, Radical Stories in the Kirstenbosch National Botanical Garden: Emergent Ecologies' Challenges to Colonial Narratives and Western Epistemologies, Environ. Humanit. 13 (2021) 66–92. https://doi.org/10.1215/22011919-8867208.

[6] F. Giorgi, Climate change hot-spots, Geophys. Res. Lett. 33 (2006). https://doi.org/10.1029/2006GL025734.

[7] F. Giorgi, P. Lionello, Climate change projections for the Mediterranean region, Glob. Planet. Change 63 (2008) 90–104. https://doi.org/https://doi.org/10.1016/j.gloplacha.2007.09.005.

[8] H. Paeth, G. Vogt, A. Paxian, E. Hertig, S. Seubert, J. Jacobeit, Quantifying the evidence of climate change in the light of uncertainty exemplified by the Mediterranean hot spot region, Glob. Planet. Change 151 (2017) 144–151. https://doi.org/https://doi.org/10.1016/j.gloplacha.2016.03.003.

[9] L. Buyun, A. Prokopiv, Rescue of unique Collections in the Botanical Gardens of Ukraine during the War, in: C. Gröschel, B. Knickmann, J.F. Hämmerle, A. Berger, M. Kiehn, D. Rohrauer (Eds.), 2nd Int. Congr. Hist. Bot. Gard., Grüne Schatzkammer, 2024. https://www.historicalbotanicalgardens.com/program/topics/ (accessed September 5, 2024).

[10] F. Fráter, T. Földi, History hidden in annual Rings, in: C. Gröschel, B. Knickmann, J.F. Hämmerle, A. Berger, M. Kiehn, D. Rohrauer (Eds.), 2nd Int. Congr. Hist. Bot. Gard., Grüne Schatzkammer, 2024. https://www.historicalbotanicalgardens.com/wp-content/uploads/abstracts.pdf.

[11] O. Hotimah, P. Wirutomo, H.S. Alikodra, Conservation of World Heritage Botanical Garden in an Environmentally Friendly City, Procedia Environ. Sci. 28 (2015) 453–463. https://doi.org/https://doi.org/10.1016/j.proenv.2015.07.055.

[12] J. Lian, S. Nijhuis, G. Bracken, X. Wu, X. Wu, D. Chen, Conservation and development of the historic garden in a landscape context: A systematic literature review, Landsc. Urban Plan. 246 (2024) 105027. https://doi.org/https://doi.org/10.1016/j.landurbplan.2024.105027.

[13] E. Pujades, A. Jurado, Groundwater-related aspects during the development of deep excavations below the water table: A short review, Undergr. Sp. 6 (2021) 35–45. https://doi.org/https://doi.org/10.1016/j.undsp.2019.10.002.

[14] G. Jia, M.F. Nehemy, L. Chen, X. Yu, Z. Liu, Ephemeral connectivity between trees and groundwater in a temperate forest in China, J. Hydrol. 610 (2022) 127887. https://doi.org/https://doi.org/10.1016/j.jhydrol.2022.127887.

[15] M.P. Mendes, P. Cherubini, T. Plieninger, L. Ribeiro, A. Costa, Climate effects on stem radial growth of Quercus suber L.: Does tree size matter?, Forestry 92 (2019). https://doi.org/10.1093/forestry/cpy034.

[16] C. Pereira, I. Flores-Colen, M.P. Mendes, Guidelines to reduce the effects of urban heat in a changing climate: Green infrastructures and design measures, Sustain. Dev. 32 (2024) 57–83. https://doi.org/https://doi.org/10.1002/sd.2646.

[17] D. Essam, M. Ahmed, A. Abouelmagd, F. Soliman, Monitoring temporal variations in groundwater levels in urban areas using ground penetrating radar, Sci. Total Environ. 703 (2020) 134986. https://doi.org/10.1016/J.SCITOTENV.2019.134986.

[18] M.C. Paz, F.J. Alcalá, J.M. Carvalho, L. Ribeiro, Current uses of ground penetrating radar in groundwater-dependent ecosystems research, Sci. Total Environ. 595 (2017). https://doi.org/10.1016/j.scitotenv.2017.03.210.

[19] M. Amato, B. Basso, G. Celano, G. Bitella, G. Morelli, R. Rossi, In situ detection of tree root distribution and biomass by multi-electrode resistivity imaging, Tree Physiol. 28 (2008) 1441–1448. https://doi.org/10.1093/treephys/28.10.1441.

[20] M.O. Cimpoiaşu, O. Kuras, T. Pridmore, S.J. Mooney, Potential of geoelectrical methods to monitor root zone processes and structure: A review, Geoderma 365 (2020) 114232. https://doi.org/10.1016/J.GEODERMA.2020.114232.

[21] Y. Giambastiani, A. Errico, F. Preti, E. Guastini, G. Censini, Indirect root distribution characterization using electrical resistivity tomography in different soil conditions, Urban For. Urban Green. 67 (2022) 127442. https://doi.org/https://doi.org/10.1016/j.ufug.2021.127442.

[22] R.S. Majewski, J. Valenta, P. Táborík, J. Weger, A. Kučera, Z. Patočka, J. Čermák, Geophysical imaging of tree root absorption and conduction zones under field conditions: a comparison of common geoelectrical methods, Plant Soil 481 (2022) 447–473. https://doi.org/10.1007/s11104-022-05648-2.

[23] W. Nijland, M. van der Meijde, E.A. Addink, S.M. de Jong, Detection of soil moisture and vegetation water abstraction in a Mediterranean natural area using electrical resistivity tomography, CATENA 81 (2010) 209–216. https://doi.org/10.1016/J.CATENA.2010.03.005.

[24] J. Vanderborght, J.A. Huisman, J. van der Kruk, H. Vereecken, Geophysical Methods for Field-Scale Imaging of Root Zone Properties and Processes, in: Soil–Water–Root Process. Adv. Tomogr. Imaging, John Wiley & Sons, Ltd, 2013: pp. 247–282. https://doi.org/https://doi.org/10.2136/sssaspecpub61.c12.

[25] J. Fäth, J. Kunz, C. Kneisel, Monitoring spatiotemporal soil moisture changes in the subsurface of forest sites using electrical resistivity tomography (ERT), J. For. Res. 33 (2022) 1649–1662. https://doi.org/10.1007/s11676-022-01498-x.

[26] T. Zhao, Y. Wang, Statistical Interpolation of Spatially Varying but Sparsely Measured 3D Geo-Data Using Compressive Sensing and Variational Bayesian Inference, Math. Geosci. 53 (2021) 1171–1199. https://doi.org/10.1007/s11004-020-09913-x.

[27] A. Gribov, K. Krivoruchko, Empirical Bayesian kriging implementation and usage, Sci. Total Environ. 722 (2020). https://doi.org/10.1016/j.scitotenv.2020.137290.

[28] L. Ansari, W. Ahmad, A. Saleem, M. Imran, K. Malik, I. Hussain, H. Tariq, M. Munir, Forest Cover Change and Climate Variation in Subtropical Chir Pine Forests of Murree through GIS, Forests 13 (2022). https://doi.org/10.3390/f13101576.

[29] V. Boumpoulis, M. Michalopoulou, N. Depountis, Comparison between different spatial interpolation methods for the development of sediment distribution maps in coastal areas, Earth Sci. Informatics 16 (2023) 2069–2087. https://doi.org/10.1007/s12145-023-01017-4.

[30] C.H.R. Lima, H.H. Kwon, Y.T. Kim, A Bayesian Kriging model applied for spatial downscaling of daily rainfall from GCMs, J. Hydrol. 597 (2021). https://doi.org/10.1016/j.jhydrol.2021.126095.

[31] E.A. Njoku, P.E. Akpan, A.E. Effiong, I.O. Babatunde, The effects of station density in geostatistical prediction of air temperatures in Sweden: A comparison of two interpolation techniques, Resour. Environ. Sustain. 11 (2023). https://doi.org/10.1016/j.resenv.2022.100092.

[32] L. Wang, R. Liu, J. Liu, Y. Qi, W. Zeng, B. Cui, A novel regional-scale human health risk assessment model for soil heavy metal(loid) pollution based on empirical Bayesian kriging, Ecotoxicol. Environ. Saf. 258 (2023). https://doi.org/10.1016/j.ecoenv.2023.114953.

[33] G. Pellicone, T. Caloiero, G. Modica, I. Guagliardi, Application of several spatial interpolation techniques to monthly rainfall data in the Calabria region (southern Italy), Int. J. Climatol. 38 (2018) 3651–3666.

https://doi.org/10.1002/joc.5525.

[34] C.A. Garcia, Apresentação. Jardim Botânico de Lisboa, in: D. Espírito-Santo, A.C. Tavares, A. Crespi, A. Gouveia, C. Lobo, C. Freitas, C. Garcia, I. Frias, J. Tinoco, J. Carrola, J. Melo, J. Capelo, L. Gouveia, M.A. Martins-Loução, M.C. Duarte, M.T.G. Cruz, P. Farinha-Marques, P. Arsénio, R. Fraga, S. Mesquita (Eds.), Jard. Botânicos Port. o Antes e o Depois 2020, ISAPress, 2021: pp. 18–19. http://hdl.handle.net/10400.5/23417.

[35] M.C. Paz, S. A.P. Santos, R. Barreira, Processing of high-resolution temporal climate data for daily simulations of a complex agro-ecosystem., Rev. Estud. Andaluces 42 (2021) 202–219. https://doi.org/10.12795/rea.2021.i42.10.

[36] GEOTEST, Limiasur, S.A. Rua da Alegria, Nºs 76 a 104. Estudo Geológico e Geotécnico, Relatório (Limiasur, S.A. Rua da Alegria, Nos. 76 to 104 Geological and Geotechnical Study, Report), 2010.

[37] IDL, Parecer sobre eventuais alterações hidrogeológicas resultantes da implementação de caves em edifícios na rua da Alegria, Lisboa (Opinion on possible hydrogeological changes resulting from the implementation of basements in buildings in Rua da Alegria, Lis, 2018.

[38] A. Valente, Chuva em Lisboa, (2022). https://www.museus.ulisboa.pt/node/195 (accessed August 22, 2024).

[39] N.J. Cassidy, Electrical and magnetic properties of rocks, soils and fluids, in: H.M. Jol (Ed.), Gr. Penetrating Radar Theory Appl., Elsevier, Amsterdam, 2009: pp. 41–72.

[40] C. Paz, F.J. Alcalá, J.M. Carvalho, L. Ribeiro, Current uses of ground penetrating radar in groundwater-dependent ecosystems research, Sci. Total Environ. 595 (2017) 868–885. https://doi.org/https://doi.org/10.1016/j.scitotenv.2017.03.210.

[41] A.P. Annan, Chapter 1 – Electromagnetic Principles of Ground Penetrating Radar, in: 2009. https://api.semanticscholar.org/CorpusID:132463062.

[42] M. Bano, G. Marquis, B. Nivière, J.C. Maurin, M. Cushing, Investigating alluvial and tectonic features with

ground-penetrating radar and analyzing diffractions patterns, J. Appl. Geophys. 43 (2000) 33–41. https://doi.org/https://doi.org/10.1016/S0926-9851(99)00031-2.

[43] A. Neal, Ground-penetrating radar and its use in sedimentology: principles, problems and progress, Earth-Science Rev. 66 (2004) 261–330. https://doi.org/https://doi.org/10.1016/j.earscirev.2004.01.004.

[44] M.C. Paz, F.J. Alcalá, L. Ribeiro, Ground Penetrating Radar Attenuation Expressions in Shallow Groundwater Research, J. Environ. Eng. Geophys. 25 (2020). https://doi.org/10.2113/JEEG19-039.

[45] R.L. Van Dam, W. Schlager, Identifying causes of ground-penetrating radar reflections using time-domain reflectometry and sedimentological analyses, Sedimentology 47 (2000) 435–449. https://doi.org/https://doi.org/10.1046/j.1365-3091.2000.00304.x.

[46] W.M. Telford, L.P. Geldart, R.E. Sheriff, Applied Geophysics, 2nd editio, Cambridge University Press, New York, 1990.

[47] S. Uhlemann, J. Sorensen, A.R. House, P.B. Wilkinson, C. Roberts, D. Gooddy, A. Binley, J. Chambers, Integrated time-lapse geoeletrical imaging of wetland hydrological processes, Water Resour. Res. 52 (2016) 1607–1625. https://doi.org/10.1002/2015WR017932.

[48] M.H. Loke, Rapid 2-D Resistivity & IP inversion using the least-squares method, Geotomo Software, 2017. https://landviser.com/wp-content/uploads/2018/02/Res2dinvx64.pdf.

[49] G. Pellicone, T. Caloiero, G. Modica, I. Guagliardi, Application of several spatial interpolation techniques to monthly rainfall data in the Calabria region (southern Italy), Int. J. Climatol. 38 (2018) 3651–3666. https://doi.org/10.1002/joc.5525.

[50] S.D. Carrière, J. Ruffault, F. Pimont, C. Doussan, G. Simioni, K. Chalikakis, J.M. Limousin, I. Scotti, F. Courdier, C.B. Cakpo, H. Davi, N.K. Martin-StPaul, Impact of local soil and subsoil conditions on inter-individual variations in tree responses to drought: insights from Electrical Resistivity Tomography, Sci. Total Environ. 698 (2020) 134247. https://doi.org/10.1016/J.SCITOTENV.2019.134247.